J|A|C|S COMMUNICATIONS

Published on Web 06/16/2009

# Chemical Synthesis of Air-Stable Manganese Nanoparticles

James F. Bondi,[†] Karl D. Oyler,[†] Xianglin Ke,[‡,§] Peter Schiffer,[‡,§] and Raymond E. Schaak*[,†,§]

*Department of Chemistry, Department of Physics, Materials Research Institute, The Pennsylvania State University, University Park, Pennsylvania 16802*

Received February 22, 2009; E-mail: schaak@chem.psu.edu

Manganese is among the most complex magnetic elements. The most stable form of Mn metal, α-Mn, adopts an elaborate body-centered cubic structure that contains 58 atoms per unit cell.[1] The magnetic properties of Mn metal are unusual as well, with α-Mn ordering antiferromagnetically with a Néel temperature ($T_N$) of 95 K rather than ferromagnetically like most of the other magnetic elements.[2] Given its unusual structure and magnetism, Mn metal is an intriguing target for size-dependent studies. However, studies of Mn nanoparticles (NPs) have been limited because of difficulties involving synthesis and stability. The large negative reduction potentials of soluble Mn salts (e.g., $E°_{Mn2+/Mn} = -1.185$ eV vs SHE) make it impossible to generate zerovalent Mn in solution using standard reducing agents that are most often employed in colloidal syntheses.[3] The oxophilicity of Mn would also render Mn NPs highly reactive in air.

Only a few examples of Mn NPs are known, prepared using methods that include ball milling,[4] inert gas condensation,[5] and arc discharge.[6] Most of these examples contain significant crystalline oxide impurities, which complicates magnetic measurements. Chemical routes to Mn-containing NPs, such as MnP,[7] MnPt,[8] and $MnPt_3$,[9] have incorporated Mn using thermal decomposition of $Mn_2(CO)_{10}$. Attempts to prepare elemental Mn NPs using similar methods have yielded oxides, as have other chemical routes to early transition metal systems.[10] Here, we report a solution chemistry method for the synthesis of air-stable NPs of α-Mn. The chemistry, used by Zhou et al. to synthesize AuPt and AuNi NPs[11] and by our group to synthesize nonequilibrium intermetallic $Au_3M$ (M = Fe, Co, Ni) NPs,[12] uses *n*-butyllithium (*n*-BuLi) as a strong reductant that is capable of reducing $Mn^{2+}$ to zerovalent Mn in a diphenyl ether solution. Oleic acid binds strongly to a thin amorphous oxide shell that coats the α-Mn NPs, rendering them air-stable. The α-Mn NPs are paramagnetic with no observable magnetic transitions, which is in contrast to the antiferromagnetism exhibited by bulk α-Mn.

The Mn NPs were synthesized using standard air-free Schlenk and glovebox techniques. In a typical synthesis, 50 mg of $MnCl_2$ and 260 μL of oleic acid were added in an argon glovebox to 10 mL of diphenyl ether in a three-neck round-bottom flask with a condenser, thermometer adapter, and rubber septum. In a separate Schlenk flask, 5 mL of diphenyl ether were mixed with 3.0 mL of 1.6 M *n*-BuLi in hexanes and capped with a rubber septum. Once prepared, both flasks were removed from the glovebox and connected to a Schlenk line under ultrahigh purity Ar. The metal salt solution was then heated to 200 °C, and the *n*-BuLi solution was injected. (Prior to this, the hexanes were removed from the *n*-BuLi solution by vacuum to prevent dangerous overpressure during injection.) Almost instantly, the solution turned from a blue-gray color to black. The solution was stirred for 20 min and then removed from the heat. All workup and product isolation procedures were performed in the glovebox.

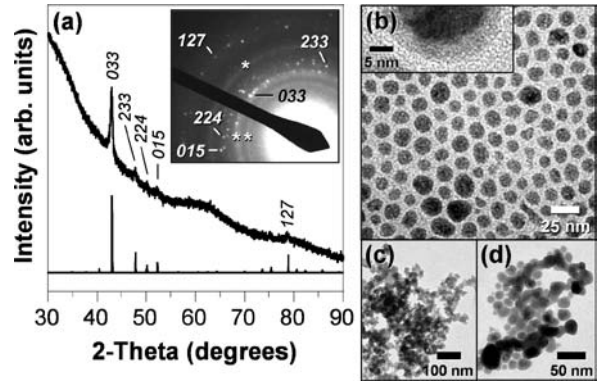


***Figure 1.*** (a) Experimental (top) and simulated (bottom) powder XRD patterns for α-Mn. The broad feature near 60° corresponds to the sample holder. Inset: SAED pattern, showing crystalline spots (indexed) consistent with the α-Mn core and diffuse rings (*) attributed to the amorphous MnO shell. TEM images of α-Mn NPs capped with (b) oleic acid (inset shows oxide shell) and (c) oleylamine and (d) α-Mn NPs (oleic acid) using a lower *n*-BuLi injection temperature.

Powder X-ray diffraction (XRD) data for the isolated product (Figure 1a) show crystalline α-Mn with no evidence of crystalline manganese oxides, which have been present in other reported examples of Mn NPs.[4,6] Scherrer analysis of the XRD data indicates an average grain size of 11 nm. Figure 1b shows a representative transmission electron microscope (TEM) image of the α-Mn NPs, which exist as spherical 13.1 ± 3.3 nm particles. The selected area electron diffraction (SAED) pattern in Figure 1a confirms that the NPs are crystalline α-Mn with diffuse rings that match amorphous MnO. A size distribution histogram (Figure S1) shows that the NPs are reasonably uniform, although not rigorously monodisperse. Other stabilizers, such as oleyl amine and trioctylphosphine, also yield nanocrystalline α-Mn, but with less desirable morphologies (Figure 1c). Optimal conditions involve the injection of *n*-BuLi at 200 °C; below this temperature, irregularly shaped α-Mn particles form (Figure 1d). Above 200 °C, oxidation is uncontrollable, and the predominant products are manganese oxides. This is likely due to decomposition of oleic acid and incorporation of its oxygen atoms into the manganese.

The α-Mn NPs appear to be air-stable, exhibiting no change in the XRD pattern or other observable properties when samples are analyzed both before and after air exposure. Figure 2a shows X-ray photoelectron spectroscopy (XPS) data for the Mn 2p core level region. After correcting for chemical shift using the C 1s peak at 284.6 eV, the XPS spectrum shows a broad Mn 2p3/2 peak at 641.2 eV and Mn 2p1/2 peak at 652.9 eV. Based on the Mn 2p3/2 and 2p1/2 peak positions and comparison with previous XPS studies of manganese oxides,[13] the surface of the NPs consists of an

[†] Department of Chemistry.
[‡] Department of Physics.
[§] Materials Research Institute.



10.1021/ja901372q CCC: $40.75 

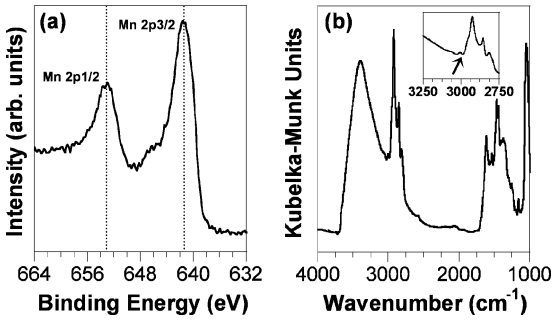


***Figure 2.*** (a) XPS spectrum of α-Mn NPs showing the Mn 2p region (referenced to C 1s peak, 284.6 eV). (b) DRIFT spectrum of oleate-coated α-Mn NPs. The expanded region in the inset highlights the observed *cis* C−H stretch at 3006 $cm^{-1}$ from the bound oleate ion.

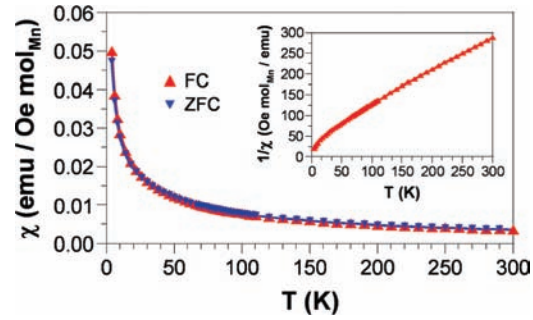


***Figure 3.*** Temperature-dependent magnetic susceptibility data (FC and ZFC) of α-Mn particles at an applied field of 100 Oe. Inset: Curie−Weiss plot with an extrapolated Weiss temperature of approximately −70 K.

oxidized shell, although it is difficult to unambiguously distinguish among the MnO, $Mn_2O_3$, and $Mn_3O_4$ oxides. However, the peak shapes (including the satellites at 644.1 and 656.5 eV) are similar to those in previously reported spectra for MnO.[13b] The presence of surface oxide is consistent with the SAED data in Figure 1, showing amorphous MnO. HRTEM images (Figures 1b, S3) confirm the presence of a 3−4 nm amorphous oxide shell, as well as the crystalline Mn core based on observation of the characteristic {033} and {220} lattice planes.

The diffuse reflectance infrared Fourier transform (DRIFT) spectrum in Figure 2b shows evidence of a *cis* C−H stretch at 3006 $cm^{-1}$, indicating that oleic acid is present.[14] However, the DRIFT spectrum does not show the peak for the corresponding COOH group at ∼1740 $cm^{-1}$ but does indicate the asymmetric stretching mode of the $COO^-$ ion between 1650 and 1400 $cm^{-1}$. This is in agreement with other metal oleates studied by DRIFT[14] and indicates that the oleic acid was deprotonated and attached to the surface of the α-Mn NPs as the oleate ion. Taken together, the XPS, SAED, and DRIFT data imply that the α-Mn NPs are capped with a thin layer of amorphous manganese oxide, to which the oleate ion is bound. This thin oxide shell and the tightly bound molecular stabilizer are likely to be responsible for the air stability of the α-Mn NPs.

Bulk α-Mn is antiferromagnetic with $T_N = 95$ K.[2] Temperature-dependent magnetization data for a commercial sample of bulk α-Mn also showed ferromagnetism corresponding to a $Mn_3O_4$ impurity, as has been observed for nanoscopic Mn prepared using ball milling[4] and arc discharge.[6] In contrast, the air-stable chemically synthesized α-Mn NPs with an amorphous oxide shell are paramagnetic with no evidence of magnetic ordering down to 4 K. Figure 3 shows temperature-dependent field-cooled (FC) and zero-field-cooled (ZFC) magnetic susceptibility data for a sample of uniform α-Mn NPs. The absence of a bifurcation between the FC and ZFC curves indicates that the α-Mn NPs are not superparamagnetic. The magnetic susceptibility data are also consistent with no crystalline oxides being present, since the features expected for these phases (e.g., superparamagnetism or magnetic ordering transitions)[15] are not observed. The paramagnetism could arise from the thin amorphous oxide shell coating the particles or from the manganese itself. The Weiss temperature derived from high-temperature Curie−Weiss fits to multiple samples is approximately −70 K. This, coupled with the fact that a magnetic phase transition is not observed down to 4 K, indicates antiferromagnetic spin−spin exchange interactions and possible large magnetic frustration, which has been reported in bulk Mn,[1] or finite size effects suppressing the magnetic ordering. Because of the large paramagnetic signal, however, we cannot exclude the possibility of an antiferromagnetic transition among a small fraction of the Mn moments.

In conclusion, NPs of α-Mn have been synthesized using a solution chemistry route. A thin amorphous manganese oxide shell and oleic acid capping groups help to stabilize the paramagnetic NPs. Given the unique attributes of Mn, this synthetic achievement and preliminary investigation of the magnetic properties is likely to provide an important foundation for future studies.

**Acknowledgment.** This work was supported by the U.S. Department of Energy (DE-FG02-08ER46483), a Beckman Young Investigator Award, a DuPont Young Professor Grant, a Sloan Research Fellowship, a Camille Dreyfus Teacher-Scholar Award, and the Petroleum Research Fund (administered by the American Chemical Society). X.K. and P.S. thank the Penn State MRSEC (DMR-0820404) and NSF (DMR-0701582) for funding. TEM imaging was performed in the Electron Microscopy Facility of the Huck Institutes of the Life Sciences and in the Materials Characterization Facility at the Penn State Materials Research Institute. The authors acknowledge use of facilities at the PSU site of the NSF NNIN. The authors also thank Tad Daniel for acquiring the XPS data, Josh Stapleton for collecting the DRIFT data, and Nam Hawn Chou for helpful discussions.

**Supporting Information Available:** Experimental details and additional microscopy and magnetometry data. This material is available free of charge via the Internet at http://pubs.acs.org.

## References

(1) Hobbs, D.; Hafner, J.; Spisak, D. *Phys. Rev. B* **2003**, *68*, 014407.
(2) Patrick, L. *Phys. Rev.* **1954**, *93*, 370.
(3) (a) Cushing, B. L.; Kolesnichenko, V. L.; O'Connor, C. J. *Chem. Rev.* **2004**, *104*, 3893. (b) Wiley, B.; Sun, Y.; Xia, Y. *Acc. Chem. Res.* **2007**, *40*, 1067.
(4) Abdul-Razzaq, W.; Wu, M. *Superlattices Microstruct.* **2001**, *29*, 273.
(5) Ward, M. B.; Brydson, R.; Cochrane, R. F. *J. Phys.: Conf. Ser.* **2006**, *26*, 296.
(6) Si, P. Z.; Brueck, E.; Zhang, Z. D.; Tegus, O.; Zhang, W. S.; Buschow, K. H. J.; Klaasse, J. C. P. *Mater. Res. Bull.* **2005**, *40*, 29.
(7) (a) Perera, S. C.; Tsoi, G.; Wenger, L. E.; Brock, S. L. *J. Am. Chem. Soc.* **2003**, *125*, 13960. (b) Gregg, K. A.; Perera, S. C.; Lawes, D.; Shinozaki, S.; Brock, S. L. *Chem. Mater.* **2006**, *18*, 879.
(8) Ono, K.; Okuda, R.; Ishii, Y.; Kamimura, S.; Oshima, M. *J. Phys. Chem. B* **2003**, *107*, 1941.
(9) Lee, D. C.; Ghezelbash, A.; Stowell, C. A.; Korgel, B. A. *J. Phys. Chem. B* **2006**, *110*, 20906.
(10) Feldmann, C.; Jungk, H. O. *Angew. Chem., Int. Ed.* **2001**, *40*, 359.
(11) (a) Zhou, S.; Jackson, G. S.; Eichhorn, B. *Adv. Funct. Mater.* **2007**, *17*, 3099. (b) Zhou, S.; Yin, H.; Schwartz, V.; Wu, Z.; Mullins, D.; Eichhorn, B.; Overbury, S. H.; Dai, S. *ChemPhysChem* **2008**, *9*, 2475.
(12) Vasquez, Y.; Luo, Z.; Schaak, R. E. *J. Am. Chem. Soc.* **2008**, *130*, 11866.
(13) (a) Audi, A. A.; Sherwood, P. M. A. *Surf. Interface Anal.* **2002**, *33*, 274. (b) DiCastro, V.; Polzonetti, G. *J. Electron Spectrosc. Relat. Phenom.* **1989**, *48*, 117. (c) Foord, J. S.; Jackman, R. B.; Allen, G. C. *Philos. Mag. A* **1984**, *49*, 657.
(14) Lee, D. H.; Condrate, R. A. *J. Mater. Sci.* **1999**, *34*, 139.
(15) Seo, W. S.; Jo, H. H.; Lee, K.; Kim, B.; Oh, S. J.; Park, J. T. *Angew. Chem., Int. Ed.* **2004**, *43*, 1115.

JA901372Q